H-2 NMR Study of Dynamics of Benzene-d(6) Interacting with Humic and Fulvic Acids

ARTICLE *in* THE JOURNAL OF PHYSICAL CHEMISTRY A · APRIL 2011

Impact Factor: 2.69 · DOI: 10.1021/jp111079s · Source: PubMed

3 AUTHORS, INCLUDING:

Margaret A Eastman
Oklahoma State University - Stillwater
29 PUBLICATIONS **790** CITATIONS
SEE PROFILE

Lucinda Brothers
Wichita State University
2 PUBLICATIONS **41** CITATIONS
SEE PROFILE

THE JOURNAL OF PHYSICAL CHEMISTRY A

ARTICLE

pubs.acs.org/JPCA

^{2}H NMR Study of Dynamics of Benzene-d_6 Interacting with Humic and Fulvic Acids

Margaret A. Eastman,*[,†] Lucinda A. Brothers,[‡] and Mark A. Nanny[§]

[†]Department of Chemistry, Oklahoma State University, Stillwater, Oklahoma 74078-0447, United States

[‡]Department of Chemistry and Biochemistry, University of Oklahoma, Norman, Oklahoma 73019-3051, United States

[§]School of Civil Engineering and Environmental Science, University of Oklahoma, Norman, Oklahoma 73019-0631, United States

ABSTRACT: Samples of three humic acids and one fulvic acid with 1% loading of benzene-d_6 in sealed glass tubes have been studied with solid-state deuterium quadrupole-echo nuclear magnetic resonance spectroscopy. Calculated spectra combining three motional models, two isotropic models and a third more restricted small-angle wobble (SAW) motional model, are fit to the experimental spectra. One isotropic motion (ISO_v) is assigned to vaporous benzene-d_6 due to the small line width, short T_1, and the loss of this component by about −25 °C when the temperature is lowered. The remaining two motional components, ISO_s and SAW, are sorbed by the humic or fulvic acid. Benzene-d_6 slowly interacts with the humic substances, progressively filling SAW sites as ISO_s motion diminishes. Both the sorption and increase in percentage of SAW motion are for the most part complete within 200 days but continue to a lesser extent over a period of a few years. For the SAW motion there are at least two and most likely a series of T_1 values, indicating more than one adsorption environment. Enthalpies of sorption, obtained from application of the van't Hoff equation to the percentages of the different motional models derived from a series of variable temperature spectra, are comparable in magnitude to the enthalpy of vaporization of benzene. In Leonardite humic acid, ΔH and ΔS for the ISO_s to SAW transition change from positive to negative values with age, implying a transition in the driving force from an entropic effect associated with expansion and deformation in the molecular structure of the humic substance to accommodate benzene-d_6 to an enthalpic effect of strong benzene-d_6—humic substance interactions. In contrast, at advanced ages, Suwannee River humic and fulvic acids have small positive or near zero ΔH and positive ΔS for the ISO_s to SAW transition.

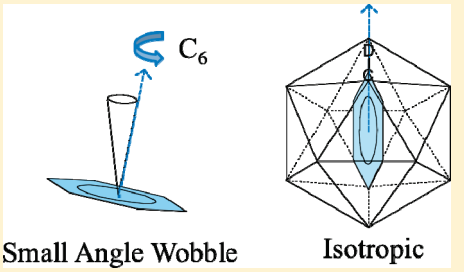

INTRODUCTION

Humic and fulvic acids (HA and FA) are two forms of humic substances (HS) naturally present in soil, sediment, and aquatic organic matter.[1−3] Because humic substances are formed through microbial and abiotic degradation of biomolecular precursors such as lignin, lipids, proteins, and polysaccharides, followed by the condensation of these degradation products,[4] they have highly heterogeneous molecular structures,[1,5] are polydisperse,[6−8] and possess a variety of functional groups including both aliphatic and aromatic structures.[3,9]

Interactions of pollutant organic chemicals with humic substances are varied and affect the fate of these organic molecules in the environment, including degradation, transport, and bioavailability.[1−3] Hydrophobic organic compounds minimally associate with the soil mineral components, sorbing mainly to humic substances.[10,11] Sorption of small organic molecules has frequently been studied for soils or humic substances in water, so that the discussion of sorption has been heavily influenced by the concept of partitioning, in which the sorbate is considered to distribute between the aqueous phase and the penetrable humic substance matrix.[2,12] Partitioning models that assume a homogeneous solid phase are not universally applicable and have given way to dual models often involving a structural model of natural organic matter with both rubbery and glassy regions that are capable of accounting for such complications as slow desorption, nonlinear sorption, and hysteresis.[12−14] Generally, rubbery, flexible, or amorphous regions of humic substance are considered to dissolve or absorb small hydrophobic molecules through a relatively rapid, linear sorption process, while in glassy, more rigid regions of humic substance the molecules adsorb or fill nanometer-sized holes more slowly in a nonlinear fashion.[10,11,13,14] The time scale of sorption and desorption equilibrium in soil may be of the order of weeks or many months, possibly explained by slow diffusion through natural organic matter[15] and slow hole-filling in glassy phases.[10] Sorption studies of solid humic substances surrounded by gas phase have determined the limiting sorption capacity of Sanhedron soil humic acid for benzene and other molecules,[16] and HA/air partitioning coefficients for sorption of a variety of polar and nonpolar organic compounds in Leonardite humic acid[17] and various humic and fulvic acids.[18]

For the past three decades, solid-state ^{2}H NMR spectroscopy has been employed to study molecular dynamics in a variety of systems, including synthetic and biological polymers and smaller

Received: November 19, 2010
Revised: March 5, 2011
Published: April 01, 2011

molecules associated with solid substrates.[19−21] Anisotropy of the quadrupolar interaction leads to characteristic line shapes for static solids, which are composed of many lines representing all possible orientations with respect to the magnetic field. Motion of molecules or groups affects the line shape, and different types and rates of motion have characteristic effects. Simulated spectra, which depend upon a model for the motion, the rate of the motion, and quadrupole parameters of the system, are matched to experimental spectra to gain an understanding of the dynamics.[20,22] Temperature variations may give activation energies[20] or the binding enthalpy of a deuterated molecule to a substrate if the line shapes represent combinations of motions that can be interpreted as free and bound.[23,24]

Numerous ^{2}H NMR studies have examined the dynamics of benzene in association with a variety of solid substrates; a few examples are zeolites,[23,25] clay,[24] ion-exchange resins,[26] and polymers.[27,28] The technique has also been applied to benzene in a variety of complexes, clathrates, and inclusion compounds.[29−32] Common motions for benzene in various environments are isotropic motion, rotation about the C_6 axis, and C_6 rotation with wobbling of the axis. The only previous solid-state ^{2}H NMR study involving humic substances examined the dynamics of several deuterated hydrocarbon molecules in association with Uncompahgre humic acid.[33]

This study presents the first application of ^{2}H quadrupole-echo NMR techniques to interactions of an aromatic hydrocarbon, benzene-d_6, with humic and fulvic acids in the solid state. We examine the types of motion benzene undergoes, how the percentages of different motions change with age, the enthalpies, entropies, and one activation energy determined from variable temperature spectra, and spin−lattice relaxation time constants at room temperature. These efforts provide indirect insights into the interactions of benzene and the humic substances by reporting on the mobility of the sorbate molecules.

EXPERIMENTAL METHODS

Benzene-d_6 (99 atom % D) was obtained from Cambridge Isotope Laboratories and used as received. Humic and fulvic acids with the following catalog numbers were obtained from the International Humic Substances Society:[34] 1S104H-5, Leonardite Humic Acid Standard; 1R106H, Summit Hill Soil Humic Acid Reference; 1S101H, Suwannee River Humic Acid Standard I; and 1R101F, Suwannee River Fulvic Acid Reference.

Benzene-d_6 was loaded at 1% by weight by means of vapor deposition onto the humic and fulvic acid samples using a Varian vacuum manifold. The manifold was constructed of stainless steel components joined with ConFlat flanges and copper gaskets, had an injection port sealed with a 6 mm diameter Teflon-coated neoprene septum, and was evacuated with an Edwards Model E2M2 roughing pump and a Varian V70LP turbo pump. The manifold volume was calibrated by performing a series of benzene injections (0.1−4.0 μL) using gastight syringes calibrated to 0.05 μL (5 μL syringes) or 0.01 μL (1 μL syringe), recording the pressure using an MKS 1 Torr Baratron Model 626A absolute pressure transducer, and plotting the ideal gas curve ($\Delta P = (RT/V)\,\Delta n$), which was linear ($R^2$ = 0.998) at the low pressures involved. To prepare a sample, a 10 mm diameter NMR sample tube with 5 mm diameter stem containing an accurately weighed sample of humic or fulvic acid was connected to the manifold via an Ultratorr glass-metal connector. After evacuation of the sample tube to a pressure less than 0.001 Torr (5×10^{-6} Torr for the LHA1 sample only), the sample valve was shut and the manifold was evacuated to a pressure less than 5×10^{-6} Torr. The manifold was then closed off from the pump and benzene-d_6 was injected and subsequently condensed in the sample tube by application of a liquid nitrogen bath. The number of moles of benzene-d_6 gas introduced into the sample tube was calculated from the difference in pressures just after injection (i.e., before opening the sample valve and introducing to the HS sample) and after condensation, using the calibrated manifold volume and the ideal gas law. Prior to flame sealing the samples, 270−360 Torr of nitrogen gas was introduced. This procedure was adopted because it was observed that 10% loaded samples (not in the current study) displayed fewer artifacts and better reproducibility of variable temperature spectra with nitrogen present, and nitrogen is not expected to alter the sorption or dynamics of the benzene. Several samples containing up to 0.26 μL of benzene-d_6 and from 0 to 360 Torr of nitrogen were made in the same manner, but without humic or fulvic acid. With sample volumes of approximately 1 cm^3 or less, benzene-d_6 in the samples without HS is expected to consist entirely of vapor at 25 °C.

The partial pressure of benzene-d_6 and the amounts of benzene-d_6 in sorbed and vaporous forms were estimated by an approximate calculation using humic substance/air partitioning coefficients ($K_{i,\mathrm{HS,air}}$), which are defined as a ratio of the concentration of benzene sorbed ($C_{\mathrm{benzene,\ HS}}$) to the concentration of benzene in the surrounding medium ($C_{\mathrm{benzene,\ air}}$):

$$K_{i,\mathrm{HS,air}} = C_{\mathrm{benzene,HS}}/C_{\mathrm{benzene,air}} \quad (1)$$

We assumed ideal gas behavior for the benzene vapor, an activity coefficient equal to 1 for benzene sorbed into HS, and negligible adsorption of benzene vapor to the glass surface of the sample container; that is, the total moles of benzene loaded (n_{load}) is equal to the sum of the number of moles of sorbed (n_{s}) and vaporous benzene (n_{v}). Hence, the following equations were combined with eq 1 to solve for the amounts of sorbed and vaporous benzene and the equilibrium partial pressure:

$$C_{\mathrm{benzene,HS}} = n_{\mathrm{s}}/m_{\mathrm{HS}} \quad (2)$$

$$C_{\mathrm{benzene,air}} \cong n_{\mathrm{v}}/V \quad (3)$$

$$n_{\mathrm{load}} = n_{\mathrm{s}} + n_{\mathrm{v}} \quad (4)$$

$$P = n_{\mathrm{v}}RT/V \quad (5)$$

where m_{HS} is the mass of HS, R is the ideal gas constant, T is the temperature, P is the equilibrium partial pressure of benzene vapor, and V is the volume of the sample container minus the volume of the HS. The volume of HS was estimated by assuming a humic or fulvic acid density of 1.5 ± 0.05 g/cm^3, which is close to those determined for Suwannee River Fulvic Acid and Pahokee Peat Humic Acid by Dinar et al.[35] The number of moles of benzene-d_6 loaded, n_{load}, was calculated from the vacuum line pressure difference. $K_{i,\mathrm{HS,air}}$ for benzene at 15 °C derived from a polyparameter linear free energy relationship was used for Suwannee River Humic and Fulvic Acids.[18] $K_{i,\mathrm{HS,air}}$ for benzene at 25 °C was calculated using the van't Hoff equation with experimentally measured equilibrium partitioning coefficients at 5 and 15 °C for Leonardite HA.[17] Because $K_{i,\mathrm{HS,air}}$ has not been measured for Summit Hill Soil HA, the $K_{i,\mathrm{HS,air}}$ value for Sanhedron Soil HA at 23 ± 1 °C was used as derived from adsorption data presented in Chiou et al.[16]

Solid-state deuterium quadrupole echo NMR spectra and inversion recovery experiments for spin−lattice relaxation time constant (T_1) determination[20] were acquired at 46.2054 MHz on a Chemagnetics CMX-II 300 MHz solid-state NMR spectrometer. Spin−lattice relaxation experiments used the quadupole echo sequence element for detection for benzene-d_6-HS samples, and a 90° pulse for samples without HS. The static (nonspinning sample) ^{2}H probe was equipped with a 10 mm transceiver coil, with 90° pulse length of 2.2 μs. Spectra were collected with delays between quadrupole echo pulses, τ, of 20, 25, 40, or 50 μs, spectral width of 500 kHz, and 1024 or 4096 points. The delay between scans was typically 2.0 s for SHHA, 2.5 s for Leonardite HA samples and SRHA, and 3.5 s for SRFA, but some spectra were acquired with delays as short as 0.5 s. The number of scans varied and was generally 10800−17280 for temperatures of −25 °C and above, while 5400 scans or less were taken at lower temperatures. A typical T_1 experiment or group of variable temperature spectra was acquired in about one week. For all data collection the probe temperature was controlled to ±0.1 °C by a Chemagnetics temperature controller through combined use of cooling gas and a heater located outside and above the probe in the variable-temperature stack. For lower temperatures (−100 to −50 °C, and sometimes −25 °C), nitrogen gas cooled by liquid nitrogen was used. For temperatures from −25 to 15 °C, a FTS Systems XRII851 chiller was used with dried compressed air as the cooling gas, while at 25 °C and above, room temperature compressed air was the cooling gas. The equilibration time prior to collection of the spectra at −50 °C and below was 0.5 h, while longer equilibration times of at least 8 h were used at −25 °C and above when practical due to the use of compressed air. Series of variable-temperature spectra taken for determination of thermodynamic values were obtained using the chiller, starting at −25 °C and proceeding stepwise upward to 50 °C.

Integrals of the deuterium quadrupole echo NMR signals provided a separate method to approximately check the amount of benzene-d_6 loaded. To do this, spectra of the benzene-d_6-HS samples were taken at 25 °C with τ equal to 25 μs, 10800 scans, and delays between scans adequate for relaxation (2.0−3.5 s as noted above). A similar spectrum of 6.6 mg alanine-d_3, with 0.5 s delay between scans, allowed a factor of moles deuterium per integral unit to be calculated. (The T_1 of alanine-d_3 is 100 ms or less at room temperature.[36]) This factor was then used to translate integrals of the test samples into moles of deuterium, from which volume of benzene-d_6 was found. This method is not very accurate for a number of reasons, the most prominent being that the benzene-d_6-HS samples cannot be contained entirely within the transceiver coil, so that up to about half of the sample, but usually less, may not be detected. Humic and fulvic acids also contain free radicals,[34] and may have small amounts of paramagnetic iron, both of which could render nearby deuterium effectively invisible due to rapid relaxation.

To derive motional parameters and percentages of different motional models, experimental spectra were matched to spectra in spectral libraries calculated with the Deuterium Motional Simulation (DMS) program by fitting with the Deuterium Fitting Program (DFP).[37] Quadrupole parameters for benzene-d_6, $\chi(^2\mathrm{H})$ = 190 kHz and η_Q = 0.04, were the same used by Laaksonen et al.[38] A range of values, both smaller and larger than this, for the quadrupole coupling constant of C_6D_6 determined by experiment and calculation have appeared in the literature.[39] For the broader patterns seen here, the effect of χ would be to alter the splitting between the horns, which can also be affected by rates and angles specified for the motional model. Because we utilize the percentages of different motional models rather than rates and angles in our analysis, the choice of χ should not have a large impact on the results. Three libraries of spectra were used in the fitting. The sorbed isotropic motion (ISO_s) and vapor isotropic motion (ISO_v) libraries used the 32-site icosahedral isotropic motional model,[24,33] with AEU kinetic mode (all sites exchange, unequal rates, with the rate depending upon the jump angle between sites[37]). For the isotropic libraries, a quadrupolar asymmetry parameter of 0.00 rather than 0.04 was used. The ranges of rates were 1×10^5 to 2.62×10^7 rad/s for ISO_s and 1×10^8 to 1×10^9 rad/s for ISO_v. The 30-site 2-frame small angle wobble (SAW)[24] library, with the 3-site C_6 rotation model and 10 wobble sites, also employed the AEU kinetic mode and had wobble rates from 5×10^3 to 5×10^5 rad/s, wobble angles from 2 to 16 degrees, and C_6 rotation rates from 1×10^6 to 1×10^8 rad/s. Euler angles representing the SAW model were chosen such that the quadrupole principal axis system in each site has the z-axis along the C−D bond, x-axis in the plane of the benzene ring, and y-axis perpendicular to the plane of the ring.[22,30,40] Errors in the percentages of motional models given below are based on the noise standard deviation of each experimental spectrum and are one-half of the error provided by DFP, which is based on twice the noise standard deviation.[37]

Inversion recovery spectra were fit after inverting negative spectra so that the amplitude of each spectrum was positive. Spectra close to a null with both positive and negative intensity were rejected from the analysis. For each sample, an initial fit of all spectra using the libraries described above gave the calculated spectrum to best match each motional model, usually taken from the spectrum having the longest relaxation delay. These spectra were then used to make single-spectrum libraries for fitting all spectra in this inversion recovery experiment, thereby not allowing the motional parameters such as rates to vary in the final fitting process. This procedure was considered appropriate, because the T_1 experiment is performed at a single temperature, and rates of motion should not vary with the relaxation delay length. The total integral of the signal was multiplied by the fraction of each motional model obtained from the DFP fit to give an intensity value for that model at each delay length. This method ignores anisotropy of T_1, giving only average T_1 values for each motional component. Intensities plotted against time were fit with two equations using the KaleidaGraph program (Synergy Software): single exponential,

$$M = M_0(1 - x\exp(-t/T_1)) \quad (6)$$

and double exponential,

$$M = M_{0A}(1 - x\exp(-t/T_{1A})) + M_{0B}(1 - x\exp(-t/T_{1B})) \quad (7)$$

where the factor x, ideally two, was varied in the fitting, taking into account imperfect inversion of the signal. T_1 values and errors in the T_1 values and coefficients were obtained by a weighted fit in which the M (y-axis values) were assigned errors propagated from an estimated 5% error in the experimental signal integral and one-half the error in model percentage provided by DFP (so that model percentage error was based upon one noise standard deviation). Errors in the percentages of each T_1 value for eq 7 were propagated from errors in the coefficients. T_1 values and their errors for samples without HS

Table 1. Measured and Calculated Parameters of the Benzene-d_6-Humic Substance Samples

sample	mass humic acid (mg ± 0.5)	volume benzene-d_6[a] (μL ± 0.01)	N_2 pressure (Torr)	benzene-d_6 loading (w/w % ± 0.01)	HS/air partitioning coefficient $K_{i,HS,air}$ (L/kg$_{HS}$)	partial pressure benzene-d_6[e] (bar)	percent benzene-d_6 sorbed[e] (%)	P/P° [e,f]
LHA1	123.3	1.25	280	0.96	126[b]	0.021	94	0.17
LHA2	125.8	1.33	270	1.00	126[b]	0.023	96	0.18
LHA3	129.0	1.36	280	1.00	126[b]	0.022	95	0.17
SHHA	168.6	1.78	360	1.00	50[c]	0.054	92	0.47
SRFA	99.3	1.06	360	1.01	30[d]	0.071	73	0.90
SRHA	106.7	1.12	270	1.00	111[d]	0.024	94	0.31

[a] Measured from pressure changes on the vacuum line. [b] 25 °C, < 0.01% RH, calculated using the van't Hoff equation and equilibrium partitioning coefficient experimental data from Niederer et al.[17] [c] 23 °C, derived from Chiou et al.[16] [d] 15 °C, 98% RH.[18] [e] Calculated from the HS/air partitioning coefficients and ideal gas law. Details of measurement and calculation methods are given in the Experimental Methods. Calculations in the last three columns are at the temperatures indicated for $K_{i,HS,air}$. [f] Benzene (C_6H_6) vapor pressure at 15 °C is 0.0786 bar, at 23 °C is 0.1154 bar, and at 25 °C is 0.1261 bar, interpolated from data given by Goodwin.[41]

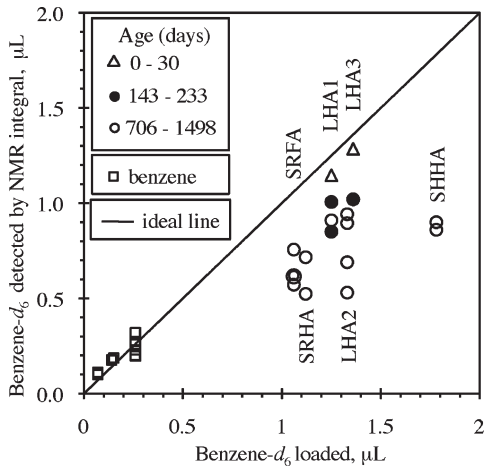

Figure 1. Volume of benzene determined from NMR integral using standard alanine-d_3 spectral integral (see Experimental Methods) is plotted against volume of benzene loaded for each 1% w/w loaded benzene-d_6-HS sample (triangles, circles), and for several samples of benzene without HS (squares). The name of each benzene-d_6-HS sample labels the column of points corresponding to its loaded amount, and ages at which the spectral integrals were obtained are indicated in the plot legend by three arbitrary categories.

were obtained by a weighted fit in which the M were assigned errors of 5% of the integral.

RESULTS

Table 1 summarizes several measured and calculated characteristics of the samples studied here, which all are within 0.04% of 1% w/w loading of benzene-d_6. With total sample volumes of about 1 cm^3 or less, the HS solid does not completely fill the sample tubes and there is some gas space. The approximate calculations made with estimated partitioning coefficients suggest that the majority of the loaded benzene-d_6 is sorbed, while the partial pressure of the vapor component (P) does not exceed the vapor pressure of benzene (P°).

Comparison of benzene-d_6 detected from the NMR signal to the quantity of benzene-d_6 loaded on the vacuum line in Figure 1 shows that signals are generally lower than expected from vacuum line loading. The NMR integral is a very rough measure of the amount of benzene because the sample tube is larger than the transceiver coil and a substantial amount of the material may be outside the coil and undetectable. Also, since the samples are not tightly packed with humic or fulvic acid, some of the variation in the values taken at different times may be due to having differing amounts of this solid material, which carries most of the signal, inside the coil. This rough correlation suggests that the actual loading is probably comparable to and at most not much greater than that indicated by the vacuum line pressure measurements.

Figure 2a shows a quadrupole echo spectrum taken of the Leonardite humic acid sample LHA2 at 25 °C 1000 days after sealing, which appears to consist of a superposition of two types of patterns: a narrow isotropic shape and a broad pattern representative of C_6 rotation or small-angle wobble (SAW) motion.[24,29] This shape is representative of most of the spectra of all samples examined. As described in the Experimental Methods and below, combinations of calculated spectra for three motional models, SAW, ISO_s (sorbed), and ISO_v (vapor), were fit to the quadrupole echo spectra of all samples using DFP.

Because pure benzene is in liquid and vapor form at 25 °C, the C_6 or SAW pattern signifies that benzene-d_6 experiences restricted motion due to its association with the humic and fulvic acids. In an initial fitting of some of the spectra, both SAW and C_6 models were tried, and it appeared that SAW fit these spectra as a group slightly better as gauged by values of R, a measure of the difference between fitted and experimental spectra;[37,42] therefore, SAW was chosen to match the broad pattern in all further fits. Differences between spectra with echo delay (τ) values of 25 and 50 μs did not assist in distinguishing between the two models; rather, spectra for both delays were generally better fit with the SAW model.

As shown in Figure 2b, the narrow central peak in the quadrupole echo spectra of LHA2 was best fit by two separate isotropic models, one broader (ISO_s) and one narrower (ISO_v). All benzene-d_6-HS samples displayed similar behavior. The sharp ISO_v peak is not due to natural abundance deuterium in either the humic or fulvic acid itself or in sorbed water, since a spectrum of an unsealed sample of Leonardite Humic Acid alone (not shown) showed no significant signal above the noise. Hence, the signal must come from a population of benzene-d_6 undergoing rapid isotropic motion. A one-pulse sequence with smaller spectral width could also be used to detect the signal representing isotropic motion while ignoring the broad SAW pattern (Figure 2c), making the two isotopic components visible, either to the eye or by deconvolution. Deconvolution of the spectrum in Figure 2c gives a ISO_s/ISO_v ratio of 60/40%, which is comparable to the 70/30% ratio determined from fitting of the

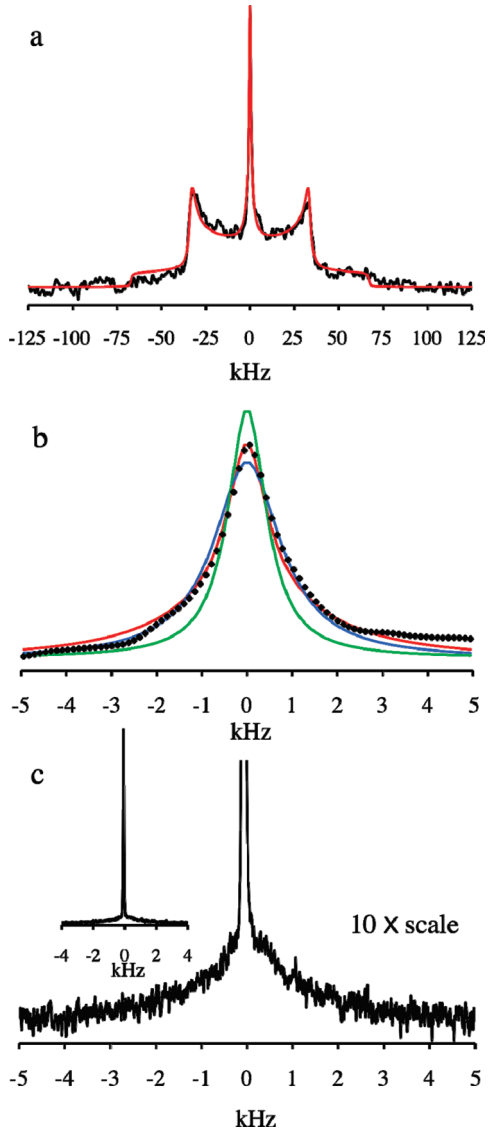

Figure 2. (a) Black trace is quadrupole echo spectrum of LHA2, aged 1000 days, at 25 °C, with 10800 scans, delay of 2.0 s between scans, τ delay of 25 μs, and 1 kHz line broadening. Red trace is calculated fit spectrum including SAW, ISO_s, and ISO_v motional models. (b) Shown in diamond symbols is the expanded center region of the spectrum in section a. Green trace is the fitted spectrum using ISO_v and SAW libraries, blue trace is the fitted spectrum using ISO_s and SAW libraries, and red trace is the fitted spectrum using ISO_s, ISO_v, and SAW libraries. (c) One-pulse spectrum of the LHA2 sample at 25 °C aged 1351 days, taken with 48000 scans, 2.5 s pulse delay, pulse width 4.8 μs, and spectral width 10 kHz, with 10 Hz line broadening applied, shows superposed broad and narrow peaks. Inset is the spectrum with the narrow peak on scale; the main plot is expanded to 10 times this scale to show the broader peak.

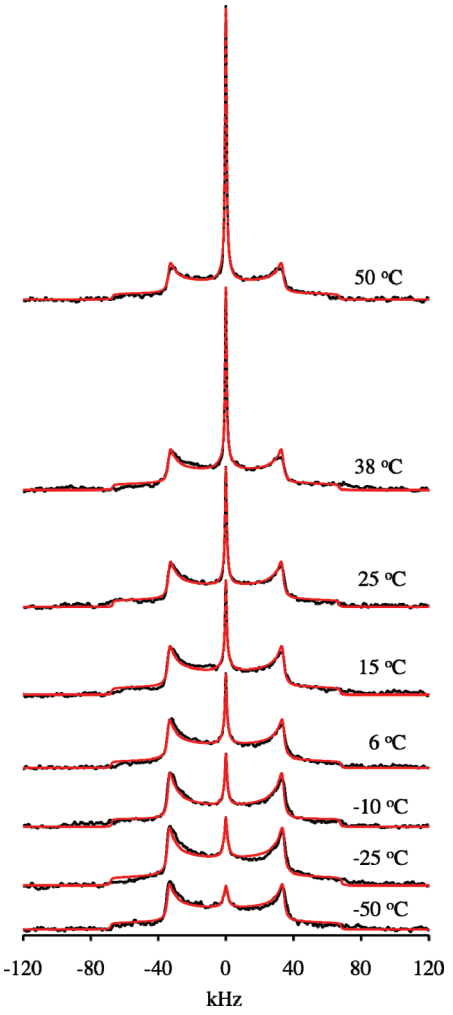

Figure 3. Variable temperature spectra of 1% w/w benzene-d_6 loaded Summit Hill Soil Humic Acid (SHHA) with 2.0 s delay between scans, τ of 25 μs, and 12000 scans (3600 at −50 °C). The sample age at the time of data collection for −50 °C was 984 days and for −25 to 50 °C was 1192 to 1198 days. Black trace is experimental spectrum; red trace is fit spectrum with ISO_s, ISO_v, and SAW components. Spectra are labeled with temperatures at which data were collected.

quadrupole echo spectrum of Figure 2a. Perhaps some of this difference is due to the broader ISO_s line not being well represented with the small spectral width; however, this could not be remedied by increasing the spectral width in the one-pulse experiment since this led to distortions in the spectrum due to the presence of the SAW pattern.

Variable temperature spectra and T_1 experiments were acquired for the samples LHA2, SHHA, SRFA, and SRHA at sample ages greater than 2 years and for LHA1 and LHA3 within a few weeks of making the sample and at more advanced ages. Figure 3 shows the SHHA variable temperature spectra as an example of the general appearance of these spectra for all samples. For the SAW model in the spectra of Figure 3, the wobble rate from spectral fitting is 5.0×10^3 rad/s at −25 °C and −10 °C, and 5.0×10^5 rad/s for 6 to 50 °C, and the C_6 rotation rate remains at 3.16×10^7 rad/s for −25 to 50 °C. The SAW wobble angle is the main parameter that changes with temperature, ranging from 2° at or below −25 °C to 8−10° at 50 °C for all samples. These small changes in the parameters are reflected in the similarity of the SAW pattern in the variable temperature spectra of Figure 3.

When the fitting program was provided with three calculated spectral libraries for the three models, it dropped the ISO_v model from the fit for experimental quadrupole echo spectra below −25 °C. Figure 4 shows the percentages of each motional model determined from DFP fits, plotted against temperature. The graph of percentage of ISO_v (Figure 4a) demonstrates that

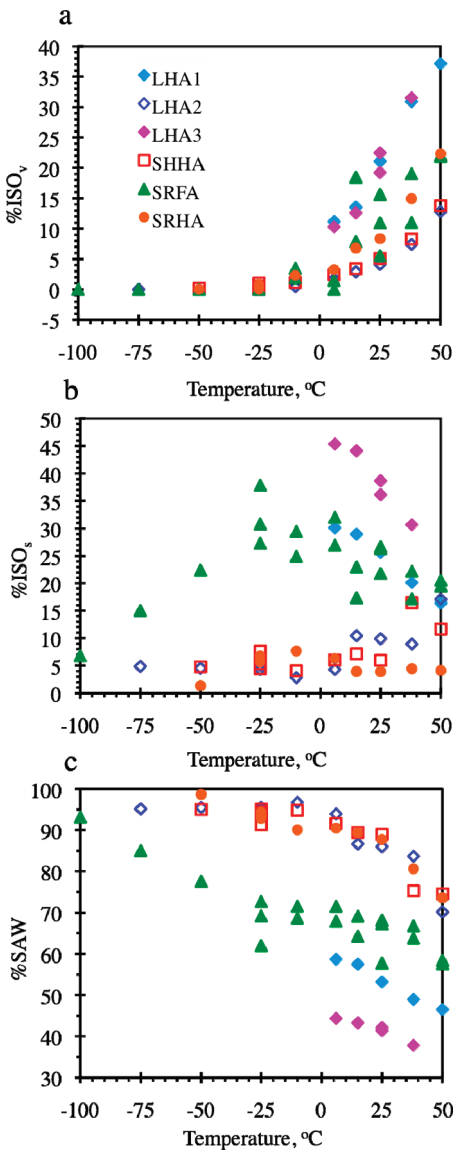

Figure 4. Percentages of motional models determined from fitting of calculated spectra to quadrupole echo spectra of 1% w/w benzene-d_6 loaded HA and FA samples taken at different temperatures: (a) % ISO_v, (b) %ISO_s, and (c) %SAW. The legend in (a) identifies the samples for all sections. Low temperature spectra below −25 °C were not obtained for LHA1 or LHA3. Data shown for samples LHA1 and LHA3 was taken at early ages (less than three months), while all other data represents advanced ages (greater than two years). Sample ages in days are LHA1, 68−72; LHA2, 1169−75 (−25 to 50 °C), 1001 and 1056 (−25 °C), 996 (−50 °C), 993 (−75 °C); LHA3, 27−33; SHHA 1192−8 (−25 to 50 °C), 1031 and 1040 (−25 °C), 984 (−25 and −50 °C); SRFA, 982 (−75 and −100 °C), 983 (−50 °C), 990 (−25 °C), 1172−8 and 1249−56 (−25 to 50 °C); SRHA, 991 (−50 °C), 991, 992, 1059, and 1063 (−25 °C), 1272−9 (−25 to 50 °C).

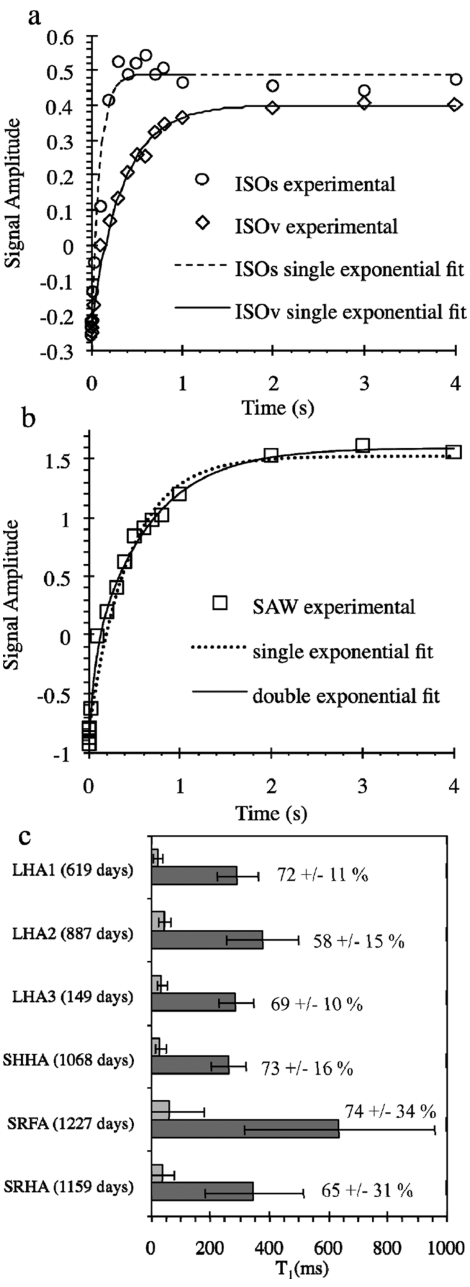

Figure 5. Fitting of spin−lattice relaxation data for SRFA sample aged 1218−27 days: (a) ISO_s and ISO_v fit with a single exponential function and (b) SAW fit with single and double exponential functions. Fit curves shown were obtained with weighting as described in the Experimental Methods. (c) Results of weighted double exponential fits for SAW motion of all samples at ages shown. For simplicity, only the percentage of the longer T_1 is shown.

essentially no ISO_v was detected at or below −25 °C for any of the four aged samples, LHA2, SHHA, SRFA, and SRHA. The smaller width of the ISO_v line and its disappearance as the temperature is lowered before loss of the ISO_s component (Figure 4b) point to an assignment of this component as benzene-d_6 vapor.

Both the ISO_s and SAW components are considered to be associated with the humic or fulvic acid. The SAW pattern must imply association with the HS, at least for spectra taken at 15 °C and above, since pure benzene would undergo only isotropic motion above the freezing point. The persistence of the ISO_s motion down to −50 °C or below suggests an association with the HS, because free benzene would most likely be frozen and experiencing C_6 rotation rather than isotropic motion at these temperatures.

Figure 3 demonstrates for SHHA a tendency shown by all the samples for the relative amounts of isotropic motion to increase,

dx.doi.org/10.1021/jp111079s |J. Phys. Chem. A 2011, 115, 4359–4372

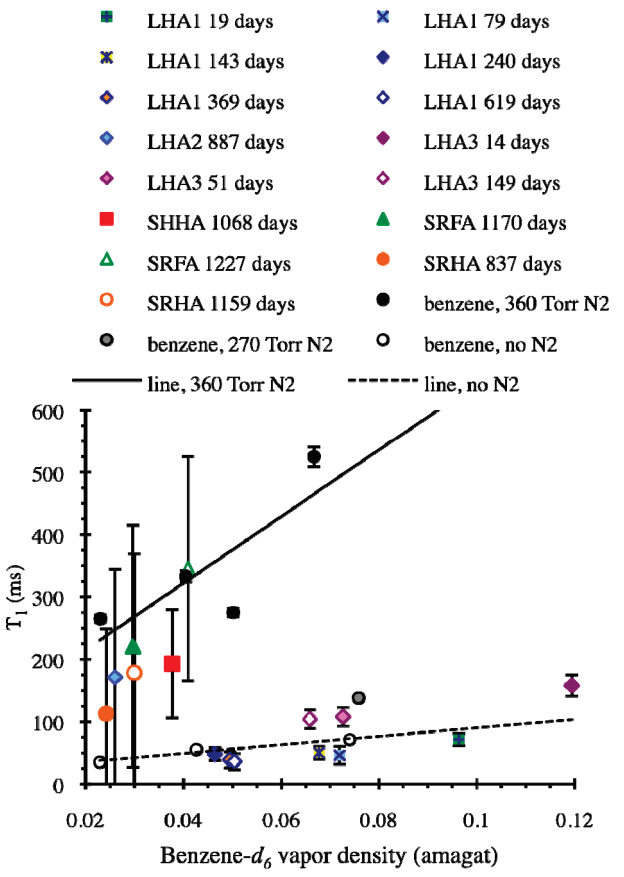

Figure 6. T_1 values at 25 °C for the ISO_v component of benzene-d_6-HS are plotted against benzene-d_6 vapor density in amagat, determined from the amount of benzene loaded and the percentage of ISO_v from the DFP fit of the inversion recovery spectrum with the longest delay. Symbols are assigned to sample names and ages in the legend. T_1 values for samples of benzene-d_6 alone (open black circles) and benzene-d_6 with added nitrogen gas (filled black circles, 360 Torr N_2; gray filled black circle, 270 Torr N_2) are also included. Lines are fit through the points for pure benzene (dotted) and benzene with 360 Torr N_2 (solid) for emphasis. Error bars that are not visible are within the width of the symbol.

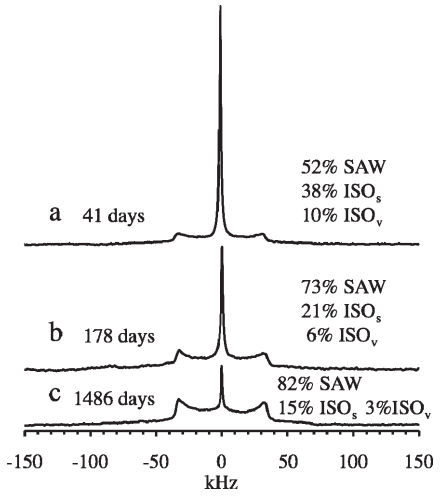

Figure 7. Deuterium quadrupole echo spectra of 1% w/w loaded benzene-d_6-Leonardite humic acid sample, LHA2, taken at 25 °C with (a) τ of 40 μs, pulse delay of 0.5 s, 57600 scans, sample age 41 days, scaled integral 5.8, (b) τ of 20 μs, pulse delay of 0.5 s, 21600 scans, sample age 178 days, scaled integral 6.4, (c) τ of 25 μs, pulse delay of 2.5 s, 43200 scans, sample age 1486 days, scaled integral 6.9. Spectra and integrals are scaled by multiplication by a factor of 21600 divided by the number of scans.

and SAW to decrease, with increasing temperature. This trend is further analyzed in Figure 4a,b with respect to the two isotropic components. Figure 4a shows that $\%ISO_v$ increases with temperature above 0 °C, while Figure 4c shows an opposite trend of decreasing %SAW with increasing temperature in the same range; both trends apply to all samples. In contrast, variations in $\%ISO_s$ with increasing temperature differ among the samples (Figure 4b), with $\%ISO_s$ increasing for LHA2 and SHHA, remaining about the same for SRHA, and decreasing for the younger LHA1 and LHA3 samples and SRFA.

ISO_s rates (ranging from 4.3×10^5 to 1.2×10^7 rad/s) for most samples do not vary systematically with temperature; however, those of the SRFA sample do systematically vary. The activation energy for isotropic motion for the aged SRFA sample (982−1003 days old), obtained from an Arrhenius plot of the logarithm of the rate provided by spectral fitting against the inverse temperature, is 10 ± 1 kJ/mol. Four variable temperature spectra in the range of −25 °C to −100 °C defined the linear range for this plot. For the other samples, the isotropic activation energy could not be determined, ostensibly because there is not enough of the ISO_s component in a low enough temperature range to reveal a change in motional rate with temperature having the Arrhenius form.

In Figure 5a, the T_1 data set for SRFA is given as an example of fitting of T_1 data taken at 25 °C for the 1% w/w benzene-d_6-loaded HS samples. While ISO_s and ISO_v inversion recovery data are best fit with a single exponential (Figure 5a), T_1 data for the SAW model are not well fit with a single exponential, as judged by visual inspection, but can be better fit with a double exponential (Figure 5b). This distinction applies to all of the samples. Figure 5c shows the two T_1 values found from double exponential fits for each sample at the ages given, along with the percentage of the longer T_1. The benzene-d_6-HA samples are similar, showing about 30% of one T_1 value at about 35 ms and about 70% of the other at about 300 ms. While poorly determined, the T_1 values of the SRFA sample seem to be longer than those of the humic acid samples, but with about the same percentages. Some data for the benzene-d_6-Leonardite HA samples (not shown) suggests variation of T_1 for the SAW motion with age, but no single sample was followed over the entire time range and additional replication would be required to establish any trend. T_1 values of the ISO_s and vapor components (ISO_v) are considered below.

ISO_v T_1 is plotted against the density of benzene-d_6 vapor in Figure 6, along with T_1 values of benzene-d_6 samples without HS. Despite some variation, spin−lattice relaxation time constants for the samples without HS increase as the quantity or vapor density of benzene-d_6 increases at fixed nitrogen density. Further, samples with nitrogen gas have longer T_1 values than those without it, showing that collisions with nitrogen molecules interrupt relaxation as well. There is also a general tendency for the ISO_v component of the benzene-d_6-HS samples to show longer T_1 at higher density, especially evident in the LHA1 and LHA3 data taken at series of ages, but also supported by data of the other samples. This tendency, and the fact that the benzene-d_6-HS ISO_v T_1 values are within or close

dx.doi.org/10.1021/jp111079s |J. Phys. Chem. A 2011, 115, 4359–4372

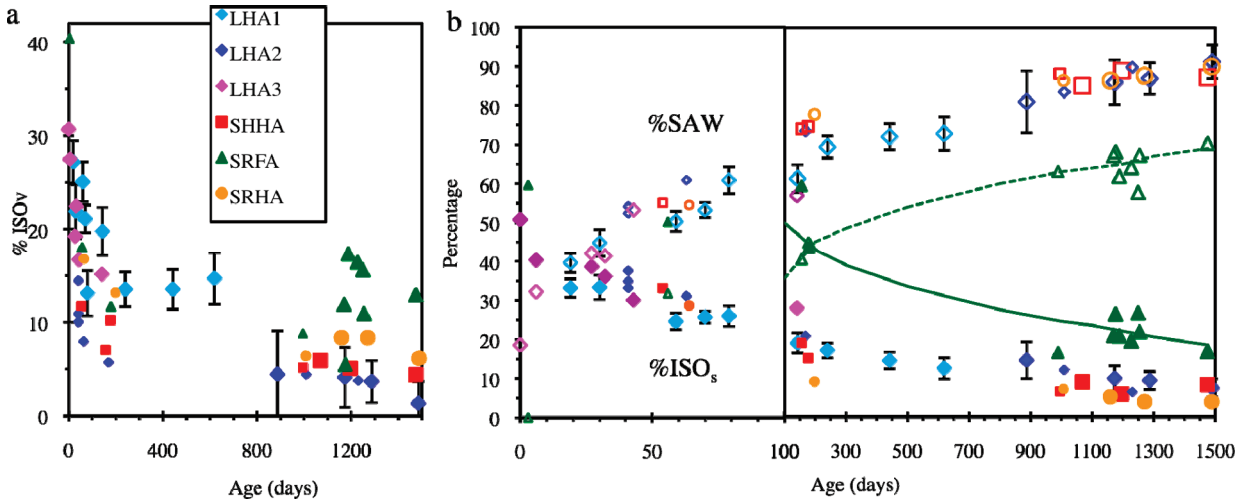

Figure 8. Percentages of motional models are plotted against sample age: (a) the percentage of ISO_v and (b) the percentages of SAW (open symbols) and ISO_s (closed symbols), from DFP fits of both quadrupole echo spectra and the last spectrum with longest relaxation delay (2−4 s) in quadrupole-echo inversion recovery T_1 experiments. All spectra were taken at 25 °C. Percentages obtained from nonquantitative quadrupole echo spectra taken with 0.5 s delays are shown with smaller symbols on both plots. Dashed line (%SAW) and solid line (%ISO) are drawn roughly near SRFA points to guide the eye in detecting the difference between SRFA and the HA samples. The graph is divided into two sections to better display the points at early ages by expansion of the *x*-axis in that region.

to the range defined by the benzene-d_6 samples without HS, provides additional support for the assignment of ISO_v to benzene-d_6 vapor. Anomalies in this data are considered below in the Discussion.

Quadrupole echo spectra taken at 25 °C of the Leonardite humic acid sample LHA2 at three different ages after sealing, each having similar signal intensity when corrected for the number of scans, are shown in Figure 7. A decrease in the percentages of both types of isotropic motion and increase in the percentage of SAW motion with time is evident from the line shape changes and the percentages derived from fitting. Percentages of ISO_s, ISO_v, and SAW from DFP fits of both quadrupole echo and quadrupole echo−inversion recovery spectra for each type of humic and fulvic acid at 25 °C are plotted against sample age in Figure 8, showing that the change apparent in Figure 7 for LHA2 is also observed for the other samples. Percentages from fits of spectra taken with 0.5 s delay between scans (smaller symbols) are also included in Figure 8, because these are the only available data at early ages for some of the samples. These points are somewhat in error because of the length of T_1 of ISO_v and SAW but are usually not far from the quantitative percentages (obtained with longer delays) at the late ages and support the increase of SAW and the decrease of ISO_s and ISO_v with age. SRFA generally has more ISO_s and less SAW over the range of ages compared to the three humic acids, which group together in Figure 8b.

Figure 9 shows how the percentages of the three motional models for the LHA1 sample aged 324−359 days recovered at 25 °C after a (−25 to 50 °C) variable temperature series. Most of the benzene-d_6 vaporized by heating to 50 °C is resorbed within two days, recovering more than half of the SAW percentage lost, and slightly increasing the ISO_s percentage. The vaporized benzene-d_6 is fully resorbed by about two weeks, and by about three weeks the ISO_s and SAW percentages have readjusted to the original values seen before heating.

Figure 10 compares percentages of ISO_v at young and old ages with the calculated percentage of vapor inferred from Table 1. For most samples, at early ages the amount of vapor detected in

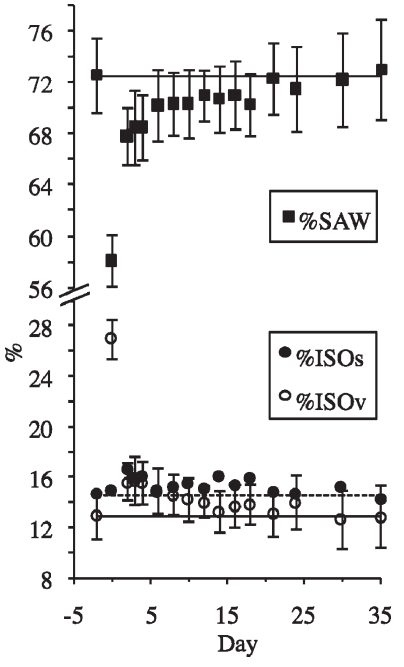

Figure 9. Recovery of percentages of the three motional models after a series of variable temperature (VT) experiments on LHA1. Points shown at −2 days represent the 25 °C spectrum taken in the VT series, which was followed by 38 °C on day −1 and 50 °C on day 0 (sample age 324 days). Points at day 0 are at 50 °C; all other points are at 25 °C. Error bars for ISO_s, which are similar to those for ISO_v, are omitted to simplify the graph. Upper horizontal line is at the −2 day value of %SAW. Lower horizontal solid (dotted) line is at the −2 day value of $\%ISO_v$ ($\%ISO_s$).

the NMR experiments is larger than the calculated amount; in contrast, at late ages the detected amount is either too small or about comparable to the calculated amount. At either age SRFA shows too little vapor and LHA1 too much vapor in comparison to the calculated percentages.

dx.doi.org/10.1021/jp111079s |*J. Phys. Chem. A* 2011, 115, 4359–4372

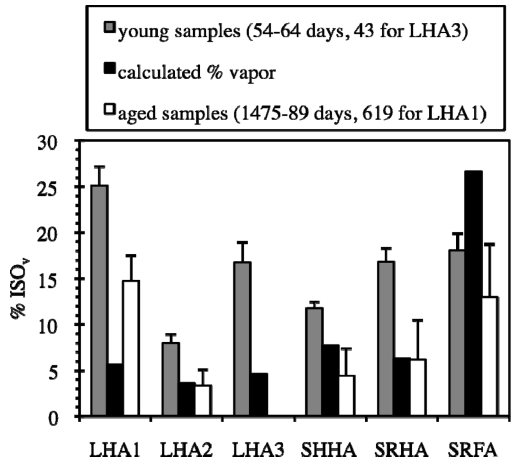

Figure 10. Bar graph comparing calculated % vapor (see Experimental Methods and Table 1) with observed % ISO_v at early and late ages. Early percentages for the LHA2, SHHA, SRFA, and SRHA samples come from spectra with 0.5 s delays and are, therefore, expected to be somewhat smaller than their real values due to incomplete relaxation.

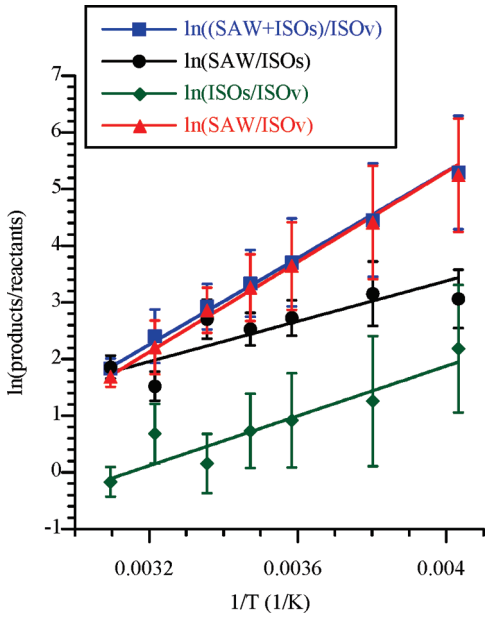

Figure 11. Shown are van't Hoff plots for ΔH and ΔS determination, corresponding to the data in Table 2, for the SHHA sample: $ISO_v \rightarrow ISO_s$ + SAW, blue squares; $ISO_s \rightarrow$ SAW, black circles; $ISO_v \rightarrow ISO_s$, green diamonds; $ISO_v \rightarrow$ SAW, red triangles.

Using the variable temperature spectra we have calculated ΔH and ΔS for the various transitions by the van't Hoff equation[24] ($\ln K = -\Delta H^\circ/RT + \Delta S^\circ/R$), plotting the logarithm of the appropriate ratios of percentages of each model from the spectral fits against the inverse temperature in the range of −25−50 °C (−10 to 6 to 50 °C for LHA1, 6−38 °C for LHA3). Figure 11 shows examples of the van't Hoff plots, and Table 2 lists the ΔH° and ΔS° values found for aged samples. The aged humic and fulvic acid samples fall into two groups with respect to the $ISO_s \rightarrow$ SAW transition: LHA1, LHA2, and SHHA, with negative ΔH and ΔS, and SRFA and SRHA, with positive ΔH and ΔS. As shown in Figure 12, the Leonardite HA samples undergo a transition with age from positive to negative ΔH and ΔS for the $ISO_s \rightarrow$ SAW transition. The above division into two groups also applies to the behavior of the ISO_s rate with age, as demonstrated in Figure 13a,b. SRFA and SRHA show considerable scatter in their ISO_s rates and no discernible trend with aging. The Leonardite HA samples and SHHA have similar ISO_s rates and experience a decrease in rate with age that is most dramatic in the first two months. For the Leonardite HA samples, a corresponding decrease in the ISO_s T_1 is seen (Figure 13c). Early T_1 values were not obtained for the other benzene-d_6-HS samples. Early spectra of the LHA2, SHHA, SRFA, and SRHA samples taken with 0.5 s pulse delay are included in Figure 13a,b under the assumption that the rates determined from spectral fitting are not significantly altered by possible incomplete relaxation in some cases.

DISCUSSION

A primary question in discussing the results shown here is whether the loading level of benzene (1% w/w) is low enough that interactions of the benzene with the HA and FA are effectively studied without the ambiguity of an excess, noninteracting liquid benzene component. Because the calculated partial pressures for the 1% loaded samples are all below the vapor pressure of benzene (Table 1), no liquid benzene should be present; all benzene should be in either sorbed or vapor phases. Hence, at this loading level, it should be possible to directly examine interactions between the humic substance and benzene, provided that the vapor signal is resolved from the sorbed signal as it has been here. Experimentally derived percentages of vapor also can be compared to those calculated from HS/air partitioning coefficients. Since the partitioning coefficients[16−18] were determined for the most part in relatively short-term experiments with equilibration times of several hours[16] or two days[17] (80-day coefficients were within 12% of 2-day ones[17]), it was anticipated that the ISO_v percentages of young samples would be closer to the calculated percentages, while the percentages in aged samples would be too small due to the slow sorption process. Instead, although calculated and experimental values are within the same order of magnitude, samples at young ages generally appear to have too much vapor in comparison to the calculated amount, while in most of the aged benzene-d_6-HA samples the percentage of ISO_v is about comparable to the calculated vapor percentage. The calculated percent vapor is only approximate because calculated or approximate values of the HS/air partitioning coefficients are used, the relative humidity for these partitioning coefficients is most likely higher than in our samples, and temperatures used for the calculations are not all 25 °C. The percentages derived from spectra also have considerable error associated with the low signal-to-noise ratio and approximate nature of the spectral calculation and fitting. Another possibility is that the ISO_v signal actually represents both vapor and free liquid benzene. However, the liquid must be present in a small amount and be exchanging rapidly with the vapor so that a single narrow line with one spin−lattice relaxation time constant represents both. This scenario seems unlikely unless the percentage of liquid is small, because the T_1 values for the ISO_v component in benzene-d_6-HS samples are comparable to those for benzene vapor, rather than an average between the benzene vapor values and the much longer T_1 of liquid benzene (1.35 s at 20 °C[38]).

The ISO_v component deserves some comment because vapor is not usually observed in ^2H spectra of deuterated molecules

dx.doi.org/10.1021/jp111079s |J. Phys. Chem. A 2011, 115, 4359–4372

Table 2. Enthalpies (kJ/mol) and Entropies (J/(mol K)) of Transitions of Benzene-d_6 in Aged Benzene-d_6-HS Samples

	transition →	ISO_v → SAW + ISO_s	ISO_s → SAW	ISO_v → ISO_s	ISO_v → SAW
sample	age (days)	ΔH	ΔH	ΔH	ΔH
LHA1	693−9	−33 ± 4	−6 ± 2	−27 ± 5	−35 ± 4
LHA2	1169−75	−37 ± 8	−16 ± 6	−22 ± 9	−39 ± 8
SHHA	1192−98	−32 ± 6	−15 ± 4	−18 ± 7	−33 ± 6
SRFA	1172−78, 1249−56	−20 ± 7	2 ± 3	−24 ± 8	−20 ± 7
SRHA	1270−77	−33 ± 6	3 ± 6	−36 ± 10	−33 ± 6
sample	age (days)	ΔS	ΔS	ΔS	ΔS
LHA1	693−9	−95 ± 13	−5 ± 9	−89 ± 17	−101 ± 12
LHA2	1169−75	−100 ± 25	−36 ± 19	−67 ± 31	−107 ± 25
SHHA	1192−98	−83 ± 19	−31 ± 13	−58 ± 23	−88 ± 19
SRFA	1172−78, 1249−56	−51 ± 24	17 ± 11	−76 ± 28	−54 ± 24
SRHA	1270−77	−93 ± 19	34 ± 21	−127 ± 33	−93 ± 19

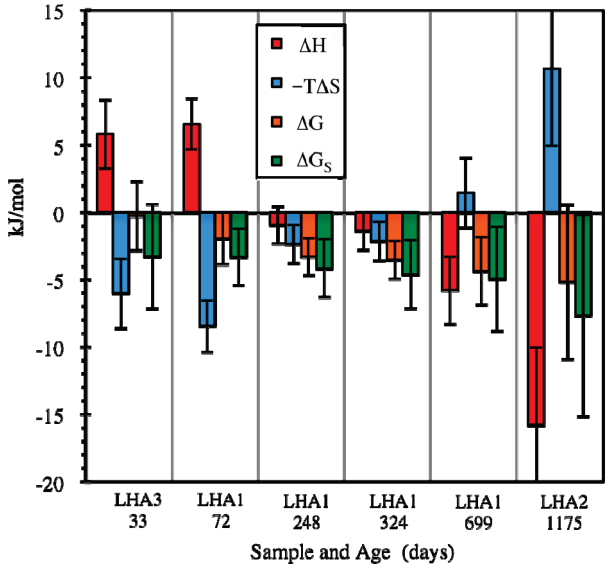

Figure 12. Graph shows variation with age in the ISO_s → SAW thermodynamic values at 25 °C for benzene-d_6-Leonardite HA samples. ΔG_S is the free energy of the sorption transition, ISO_v → ISO_s + SAW.

interacting with various substrates. Vapor is seen here because the sample tubes are not packed tightly with solid humic substance, but instead have gas space, and also because the sensitivity of detection is enhanced by the presence of six deuterons per molecule. The ISO_v line is assigned based upon its small width and behavior as the temperature is lowered, but the T_1 values are also reasonable for vaporous benzene-d_6. For example, D_2 gas has shorter T_1 values, in the ms range, in helium gas[43] than in H_2O liquid where T_1 is in the range of seconds.[44] Similarly, our ISO_v T_1 (36−345 ms for benzene-d_6-HS samples, 34−521 ms for benzene-d_6 without HS) is shorter than the T_1 of liquid benzene. Because the T_1 of a gas should depend directly on the amount of gas present[45] because collisions between gas molecules interrupt the processes that bring about relaxation,[46] a roughly linear relation of ISO_v T_1 with the density of the benzene vapor might be expected. Although it is not possible to conclude that the observed relationship of T_1 to benzene density is linear, longer T_1 values are generally associated with greater gas density for the samples without HS and those with HS (Figure 6). Examining the T_1 values for benzene-d_6 without HS at 0, 270, and 360 Torr of N_2, it is clear that the dependence of benzene-d_6 T_1 on N_2 density is not linear; rather, T_1 increases very little between 0 and 270 Torr and makes a larger step up at 360 Torr. This low sensitivity of T_1 to the N_2 density coupled with the possibility for errors in the amounts loaded, particularly for N_2, could account for the anomalously low T_1 values of the LHA1 sample. Two aged samples, LHA2 and SRHA, appear closest to the other samples with 360 Torr N_2, although their nominal N_2 content is lower. Maybe this is due to error in the T_1 measurement or error in the amount of N_2 in the sample or release of H_2O from the humic acid to the vapor phase with age.

Above the freezing point of benzene we do not attribute the ISO_s component to liquid benzene, because the T_1 values for this component (31−128 ms) are much smaller than the T_1 of liquid benzene. Similar T_1 values are observed for benzene-d_6 displaying isotropic motion in zeolites, with T_1 values of about 37 ms for Na LSX at about room temperature (76.54 MHz)[25] and 35−78 ms for NaY DAY and USY at 290 K (46.07 MHz, higher values correspond to higher loading).[47] The presence of the ISO_s component at very low temperature in SRFA (to −100 °C) and as low as −25 °C or −50 °C in the humic acid samples makes it reasonable to equate the ISO_s peak, at least below the freezing point of benzene-d_6 (6.8 °C[48]), with benzene associated with the humic or fulvic acid yet able to move about isotropically, most likely within pores. Xiong et al. observed isotropic motion of acetone-d_6 molecules (6.5 w/w%) associated with Uncompahgre humic acid at temperatures as low as −125 °C, and attributed this to isolated acetone molecules in small voids in the HA.[33] Benzene-d_6 also undergoes isotropic motion at temperatures as low as −50 °C (1.2 w/w%) and −100 °C (3.9 w/w%) in the interlayer space of Ca-montmorillonite clay.[24]

In keeping with current views of sorption by humic substances, benzene-d_6 might be dissolved in rubbery, flexible regions of the HA or FA,[49] and the possible assignment of the ISO_s motion to this dissolved benzene should be considered. For comparison, examples of isotropic motion of benzene-d_6 in association with synthetic polymers include a broad signal attributed to isotropic motion at intermediate rates in the amorphous phase of semicrystalline syndiotactic polystyrene film[28] and an isotropic doublet in stretched polyethylene.[50] However, in our samples, the single T_1 value for the ISO_s component suggests the signal does not arise both from benzene in pores and dissolved in flexible

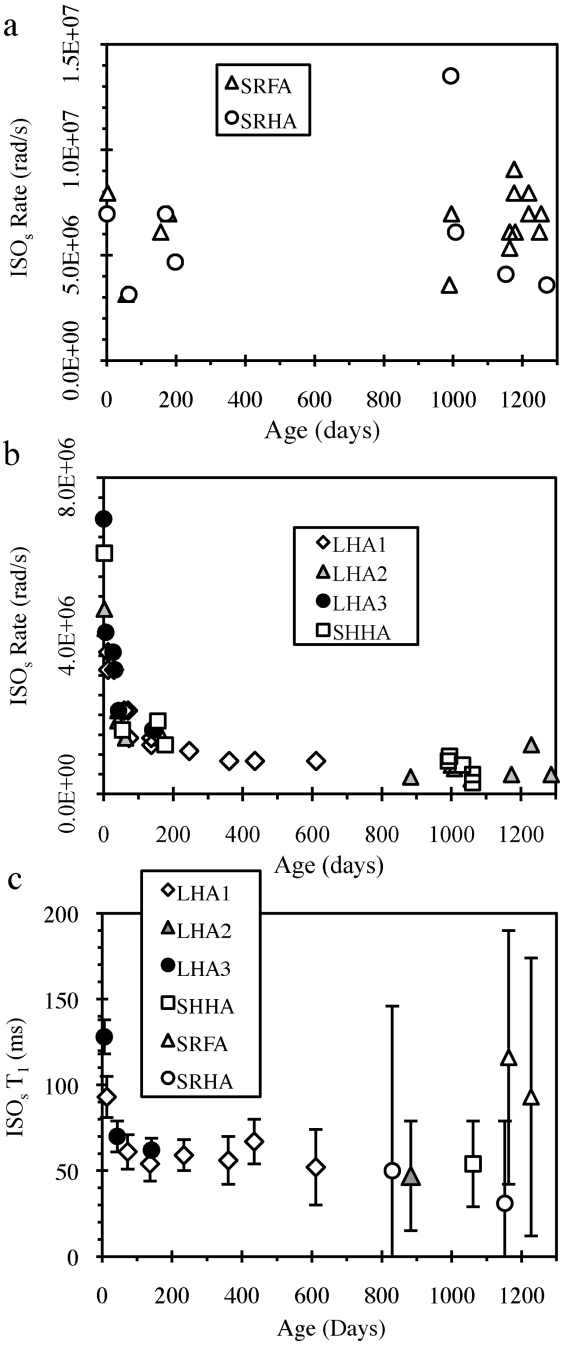

Figure 13. Rates of ISO_s motion component determined from DFP fitting are plotted against the age of the sample for (a) SRFA and SRHA, and (b) Leonardite HA samples and SHHA. Multiple points at one age, obtained either from spectra with 25 and 50 μs τ values or from the longest two delay values of T_1 experiments, give an indication of the error in the rate values. All spectra were collected at 25 °C, except the earliest points (1−2 days) for LHA2 (7 °C), SHHA (6 °C), and SRHA (0 °C). (c) ISO_s T_1 (ms) values (25 °C) plotted against sample age.

regions, which would likely have different T_1 values. Because pores are expected to be present and to be occupied by benzene, the simplest assignment of ISO_s is to benzene in pores. The ISO_s activation energy for the SRFA sample (10 ± 1 kJ/mol), comparable to the activation energy of 10.6 ± 0.9 kJ/mol found for benzene-d_6 in the zeolite Na LSX,[25] does not contradict this.

Below the freezing point, some of the SAW component may be frozen benzene not associated with the humic acid, freezing from the vapor phase; however, this should be in the minority, because the percentage of vapor at room temperature is small compared to the percentage of sorbed benzene. As mentioned previously, above the freezing point any SAW motion must imply association with the substrate, since free benzene in liquid or gas form could only have isotropic motion. Complementary to the assignment of ISO_s to benzene in voids, the more restricted SAW motion implies tighter association of the benzene-d_6 with the HS or motion within smaller spaces, and so may represent benzene interacting with a variety of different structural groups within the HS, both rubbery or flexible and glassy or rigid, as well as benzene in pores that are too small to allow isotropic motion. The HS structures may include aliphatic groups or flexible amorphous poly(methylene) domains, which have been correlated with sorption capacity for phenanthrene[51,52] and pyrene[53] in several humic substances including Leonardite humic acid,[51] and aromatic groups. As might be expected if the SAW motional component represents a range of sites, here is no correlation applying to all of the samples between percentage of SAW and aromatic or aliphatic percentage determined by ^{13}C NMR[34] (data not shown).

Although measurements of the spin−lattice relaxation time T_1 show that for all of the 1% benzene-d_6 loaded samples the sorbed benzene undergoing SAW motion can be fit with a double exponential, instead of two discrete T_1 values, it is likely that there are a series of several or many T_1 values. These disparate T_1 values may be due to association of the benzene with regions of the humic acid that have different levels of flexibility, or binding with different strengths, in keeping with the suggestion that there is a continuum of phases in humic substances extending between the extremes of rubbery, flexible, and expanded and glassy, rigid and dense, rather than simply two phases at the extremes.[10] Because the HS has a complex structure with varying composition of individual molecules that associate to form the solid material, and variety of structure in the HA would allow for different modes and strengths of binding of benzene, a range of SAW motions is more believable than two discrete populations, as implied if a double exponential were strictly correct. Given the signal-to-noise ratio and associated limitations on the number of points in the T_1 experiments presented here, it is not possible to determine whether a larger number of exponential functions would provide a better fit. Further measurements should be made with higher field strength and magic-angle spinning[54] for better sensitivity to better define the T_1 values for SAW motion.

As the early decrease in ISO_v percentage shows, complete sorption of benzene is a slow process and may still be in progress at 200 days (Figure 8). This result is in keeping with previous studies showing that sorption of organic molecules may take weeks to many months in soils, sediments, and peat.[10,15] A two-stage sorption process with the first stage in hours and the second over several days was demonstrated for small organic molecules sorbing to humic acid disks,[55] but our work may be the first to show slow sorption to humic and fulvic acids, rather than whole soils, over a period of months.

As benzene is slowly sorbed, the percentage of SAW motion gradually increases. The most sensible explanation is that, although it may quickly (within the first day) enter voids and access some more superficial SAW sites, benzene penetrates very slowly through the bulk of the humic substance, incrementally discovering or opening up more SAW sites. This is in keeping

with the explanation of slow sorption in soils by slow processes of diffusion into natural organic matter[15] and hole-filling.[10] Sorption of benzene-d_6 may cause expansion and structural deformation of glassy regions of the HA, as previously demonstrated for sorption of naphthalene on kerogenous organic matter[56] and polychlorinated benzenes on soil humic acid.[57] Regarding the dual model for sorption, the observed increase in the percentage of benzene-d_6 undergoing SAW motion over time fits well with the increase in nonlinearity of sorption to soils, associated with adsorption in glassy regions, with greater contact time between the sorbate and the soil,[10] if glassy SAW sites fill more slowly than rubbery ones. More thorough relaxation studies of the benzene in SAW motion, as proposed above, would be valuable to suggest whether SAW sites in glassy regions fill more slowly by showing changes in T_1 values as a function of age that might be indicative of changes in the range of flexibility of the SAW sites.

The thermodynamic values characterize transitions occurring within about a day, rather than the slow transformation over months to higher percentage of SAW motion. As the temperature is raised to 50 °C, some benzene-d_6 in SAW sites desorbs, but in aged samples not all benzene in SAW motion is able to leave slowly filled adsorption sites to exchange with either sorbed ISO_s or vapor on the time scale of one day. One explanation for the failure to reach complete equilibrium within a day may be that sorbed benzene-d_6 is kinetically hindered from exchanging. For example, a benzene-d_6 molecule undergoing SAW motion may have to diffuse through a rigid region in order to reach a pore where ISO_s motion is allowed, or escape to the vapor phase. A thermodynamic explanation for the inability to reach complete equilibrium is that benzene-d_6 is associated with SAW sites of varying binding strength, some of which are strong enough to require more than the available thermal energy at 50 °C to remove benzene-d_6. The observation of at least two T_1 values for SAW sites favors the thermodynamic explanation, while the presence of kinetic barriers is suggested by the long times required for completion of sorption and the longer-term $ISO_s \rightarrow$ SAW transition.

Values of ΔH and ΔS show that sorption ($ISO_v \rightarrow ISO_s$ + SAW) has a negative ΔG value at 25 °C and so is spontaneous for all the HS types studied (at advanced sample ages, and also in the young Leonardite HA samples). The similarity of thermodynamic values for the $ISO_v \rightarrow$ SAW and sorption transitions suggests that SAW is the dominant sorbed species, as Figure 8 corroborates. The enthalpy change for the sorption transition for all samples is close to the negative of ΔH of vaporization of benzene (C_6H_6), 33.83 kJ/mol at 25 °C.[58] Comparison of the values suggests that the sorption of benzene to humic and fulvic acids is for the most part comparable to or weaker than the interaction of benzene molecules with each other in the liquid. Sorption of benzene-d_6 to humic and fulvic acids is weaker than binding to Ca-montmorrillonite, with enthalpy of desorption of 42 ± 4 kJ/mol (SAW → ISO), where the proposed mechanism is formation of π-complexes with Ca^{2+}.[24] A vapor component was not detected in this work, and the isotropic motion was considered to be free benzene in the interlayer space while the SAW motion was assigned to π-complexes.[24] Similarly, the maximum differential heat of adsorption of benzene on zeolite H−Y is 66−67 kJ/mol, presumably due to interaction of benzene molecules with Bronsted acid sites.[59] Because these strong interactions of benzene with positive charges are not expected in the case of the humic and fulvic acids, but rather only weaker van der Waals interactions, the smaller enthalpy of sorption is reasonable.

For the $ISO_s \rightarrow$ SAW transformation, which is spontaneous at 25 °C, there are at least two possibilities: benzene moving physically from a pore to a SAW adsorption site at a different location within the humic substance, or benzene undergoing a transition akin to freezing, while remaining within a pore. The latter transition should have a negative enthalpy change associated with benzene adhering to the pore surface and a negative entropy change associated with decreased benzene motion, while the enthalpy and entropy changes of the former could vary depending upon the separate values of each for the rearrangement of the HS structure and the association with benzene.

For young LHA1 and LHA3 and aged SRFA and SRHA, the small positive or near zero $ISO_s \rightarrow$ SAW ΔH suggests the dominance of a transition in which benzene changes location, which requires some energy to accomplish because the HS molecular fragments need to rearrange in the process, with the entropy and enthalpy of the HS going up and more than canceling the entropy and enthalpy decreases for benzene that are necessary due to the reduced flexibility of the benzene motion and formation of a stable association with the HS. Positive changes in both entropy and enthalpy indicate an entropic driving force for the $ISO_s \rightarrow$ SAW transition stemming from increased flexibility of rigid regions in the HS molecules. In contrast, for aged LHA1, LHA2, and SHHA, negative ΔH and ΔS suggest either the dominance of an in-place freezing transition or strong binding at sites that retain a significant degree of structural rigidity and so require little rearrangement. The changes with age in ΔS for $ISO_s \rightarrow$ SAW of Leonardite HA samples do not proceed at the same rate as the changes in ΔH (Figure 12), with ΔH becoming negative by 248 days, but ΔS becoming negative by 699 days, suggesting that the transformation is not brought about by increasing dominance of an in-place freezing transition, for which both ΔH and ΔS should be negative. Strong binding would require specific noncovalent interactions, such as $\pi-\pi$ interactions between benzene and aromatic functional groups. A stabilizing enthalpic effect of 12.9 ± 4.9 kJ/mol has been reported for $\pi-\pi$ interactions of stacked phenyl rings in dibenzyl ketone,[60] which compares well with the $ISO_s \rightarrow$ SAW ΔH in aged LHA2 and SHHA (−16 ± 6 and −15 ± 4 kJ/mol, respectively).

The size of the humic substance molecules is expected to affect their interactions with other organic molecules. Due to their structural variety, polydispersity, and tendency to aggregate through hydrogen bonds and hydrophobic interactions, the determination of molecular masses of humic and fulvic acids remains an ongoing effort; however, disaggregated preparations of some HA and FA have shown molecular masses in the range of hundreds to a few thousand Daltons.[12,61] To our knowledge, disaggegated molecular masses for the samples studied here have not been determined. Literature values from size exclusion chromatography and flow field-flow fractionation suggest that the aquatic humic substances Suwannee River FA and HA (weight (M_w) and number average (M_n) molecular masses about ∼2−5 and ∼1−2 kDa, respectively[6,8]) have smaller molecular masses than Leonardite HA (M_w, M_n (kDa) = 18.7, 3.73[6]). Presumably, Summit Hill Soil HA would also have higher molecular mass, because soil humic acids tend to have higher observed molecular mass than aquatic humic or fulvic acids.[6,8] Positive values of $ISO_s \rightarrow$ SAW ΔH and ΔS at advanced sample age are associated with aquatic HS and negative values are associated with soil HS in this work. Considering the assumed molecular mass differences only, the distinction between the two

groups might be explained as follows. Larger molecular masses foster more inter- and intramolecular interactions, making the HS structure more strongly held together and less flexible. In contrast, smaller molecular masses allow for fewer such interactions, giving a structure that is more flexible to rearrangement. In the latter case, even at advanced ages, most SAW sites remain flexible enough that benzene must disrupt the HS structure for their formation, making the transition entropy driven. In the former case, at early ages benzene must disrupt the less flexible HS structure to form SAW sites, again giving an entropy-driven transition, but now also one that is endothermic due to the need to break stronger HS−HS interactions. Once the expansion and deformation of these more tightly associated regions of the HS are accomplished, the SAW sites remain even as benzene desorbs and resorbs or relocates from ISO_s sites, so that the driving force for the $ISO_s \rightarrow$ SAW transition at later ages depends mainly upon ΔG for benzene and is dominated by a favorable ΔH due to the reduction in energy from stable close association with the HS that overcomes an unfavorable entropy decrease as the motion of benzene becomes more restricted. The differences in $ISO_s \rightarrow$ SAW thermodynamic values in the two groups probably stem from differences in structure as well as molecular size, but the molecular heterogeneity of humic substances and lack of detailed structures makes it difficult to identify what the discriminating structural characteristics are. Perhaps the chemical groups present in the soil humic substances favor the formation of more glassy and inflexible regions than those in the aquatic humic substances.

There is also a lowering of the apparent rate of benzene-d_6 ISO_s motion with age for the soil HA samples, while this rate remains higher, is less well-defined, and does not vary systematically with age in the aquatic HS samples. The accompanying decrease in T_1 with age for benzene-d_6-Leonardite HA samples might be interpreted as follows. If the T_1 values are determined by motion within pores, the relaxation rate will be a weighted average of the rates for benzene free within the pore and bound to the inner surface of the pore.[62] As the size of the pore becomes smaller, the faster relaxation rate (shorter T_1) of the surface-bound species will have greater influence on the observed T_1.[62] Hence, the drop in T_1 over time for the benzene-d_6-Leonardite HA samples could be due to benzene accessing smaller pores over time, such that the average pore size decreases. The apparent ISO_s rate decrease may not be truly a decrease in the motional rate, but may instead be due to increased line broadening accompanying a slower exchange rate between the free and bound species in pores. The distinction between the soil and aquatic benzene-d_6-HS samples is then explainable by smaller sizes of less accessible pores in the higher molecular mass soil humic acids compared to more uniform larger average pore sizes in the lower molecular mass aquatic humic substances.

CONCLUSIONS

Two molecular motions of sorbed benzene-d_6 are detected in association with four types of solid phase humic and fulvic acids (Leonardite, Summit Hill Soil, and Suwannee River HA, and Suwannee River FA): isotropic motion (ISO_s), which probably represents benzene in voids within the HS, and a more restricted small angle wobble (SAW) motion, consisting of C_6 rotation and wobbling of the C_6 axis, which implies stronger association with the HS. Benzene in ISO_s motion shows only one T_1 value, while benzene in SAW motion appears to have two or more T_1 values, suggesting the presence of different restrictive-motion sorption sites within the HS. Benzene sorbs to a large extent over a period of about 200 days but continues to gradually sorb over a longer period of a few years, in keeping with slow sorption of other organic compounds observed previously in sorption studies of soils. The percentage of sorbed benzene undergoing SAW motion increases as the percentage undergoing ISO_s motion decreases over the same time period, suggesting the transfer of benzene to more thermodynamically favorable, but kinetically hindered, interactions. The magnitude of ΔH of sorption indicates benzene-d_6-HS interactions are on average comparable in strength to liquid benzene−benzene interactions, which is a reasonable observation because van der Waals interactions are the expected mode of association.

The soil humic acids are distinguished from the aquatic humic substances by the thermodynamic values for the $ISO_s \rightarrow$ SAW transition. For aged samples of benzene-d_6 with the soil humic acids, Summit Hill Soil or Leonardite HA, negative enthalpy values for the $ISO_s \rightarrow$ SAW transition can be explained by movement of benzene-d_6 from pores to structurally rigid SAW sites that are capable of noncovalent interactions such as $\pi-\pi$ bonding with benzene. In contrast, for the aged benzene-d_6-Suwannee River HA or FA samples, the $ISO_s \rightarrow$ SAW transition has a positive entropy value and very small positive or near zero enthalpy value, indicating that the driving force for the transition is entropic and increased disorder or flexibility of the HS matrix is required for the association of benzene at SAW sites. These two groups are also distinguished by the apparent rate of ISO_s motion, which decreases within the first 100 days for the soil humic acids but not for the aquatic humic substances, perhaps because less accessible pores are of smaller size in the soil humic acids. In benzene-d_6-Leonardite HA samples, for which ΔH and ΔS of the $ISO_s \rightarrow$ SAW transition have been followed with aging over a period of a few years, there is a progression from an entropic to an enthalpic driving force for the transition, indicating that over time, the entry of benzene into Leonardite HA causes a lasting disruption of the structure. All of these observations are in keeping with a structural picture in which the soil humic substances are more likely than are the aquatic humic substances to have domains that are dense, less flexible, and less likely to reorganize. This may be partially due to differences in molecular size, but may also be due to differences in chemical structure.

AUTHOR INFORMATION

Corresponding Author

*E-mail: meastman@chem.okstate.edu.

ACKNOWLEDGMENT

The authors thank Ms. Tu Pham for making the sample LHA1 and Frank D. Blum for reading the manuscript. This material is based upon work supported by the National Science Foundation under Grant No. 0210839. Any opinions, findings, and conclusions or recommendations expressed in this material are those of the authors and do not necessarily reflect the views of the National Science Foundation (NSF).

REFERENCES

(1) Stevenson, F. J. *Humic Substances in Soil, Sediment, and Water: Geochemistry, Isolation, and Characterization*; John Wiley and Sons: New York, 1985; pp 13−52.

(2) Senesi, N.; Chen, Y. *Ecological Studies 73 (Toxic Organic Chemicals in Porous Media)* **1989**, 37–90.
(3) Schnitzer, M. *Adv. Agron.* **2000**, *68*, 1–58.
(4) Tissot, B. P.; Welte, D. H. *Petroleum Formation and Occurrence*, 2nd ed.; Springer-Verlag: Heidelberg, 1984.
(5) Frimmel, F. H.; Christman, R. F, Eds. *Humic Substances and Their Role in the Environment*; John Wiley and Sons: New York, 1988.
(6) Beckett, R.; Jue, Z.; Giddings, J. C. *Environ. Sci. Technol.* **1987**, *21*, 289–95.
(7) Swift, R. S. *Soil Sci.* **1999**, *164*, 790–802.
(8) Perminova, I. V.; Frimmel, F. H.; Kudryavtsev, A. V.; Kulikova, N. A.; Abbt-Braun, G.; Hesse, S.; Petrosyan, V. S. *Environ. Sci. Technol.* **2003**, *37*, 2477–85.
(9) Hayes, M. H. B.; Malcolm, R. L. Humic Substances and Chemical Contaminants. Proceedings of a Workshop and Symposium, Anaheim, CA, United States, Oct. 26−7, 1997, Soil Science Society of America: Madison, WI, 2001; pp 3−39.
(10) Pignatello, J. J. Mineral−Water Interfacial Reactions: Kinetics and Mechanisms. *ACS Symposium Series 715*; American Chemical Society: Washington, DC, 1998; pp 204−221.
(11) Weber, W. J.; Huang, W.; Leboeuf, E. J. Mineral−Water Interfacial Reactions: Kinetics and Mechanisms. *ACS Symposium Series 715*; American Chemical Society: Washington, DC, 1998; pp 222−241.
(12) Schauman, G. E. *J. Plant Nutr. Soil Sci.* **2006**, *169*, 145–156.
(13) Xia, G.; Pignatello, J. J. *Environ. Sci. Technol.* **2001**, *35*, 84–94.
(14) Leboeuf, E. J.; Weber, W. J., Jr. *Environ. Sci. Technol.* **2000**, *34*, 3632–3640.
(15) Pignatello, J. J.; Xing, B. *Environ. Sci. Technol.* **1995**, *30*, 1–11.
(16) Chiou, C. T.; Kile, D. E.; Malcolm, R. L. *Environ. Sci. Technol.* **1988**, *22*, 298–303.
(17) Niederer, C.; Goss, K.-U.; Schwarzenbach, R. P. *Environ. Sci. Technol.* **2006**, *40*, 5368–5373.
(18) Niederer, C.; Schwarzenbach, R. P.; Goss, K.-U. *Environ. Sci. Technol.* **2007**, *41*, 6711–6717.
(19) Spiess, H. W. *Colloid Polym. Sci.* **1983**, *261*, 193–209.
(20) Griffin, R. G.; Beshah, K.; Ebelhauser, R.; Huang, T. H.; Olejniczak, E. T.; Rice, D. M.; Siminovitch, D. J.; Wittebort, R. J. *The Time Domain in Surface and Structural Dynamics*; Kluwer Academic Publishers: Norwell, MA, 1988, 81−105.
(21) Vold, R. R. *Nuclear Magnetic Resonance Probes of Molecular Dynamics*; Kluwer Academic Publishers: Norwell, MA, 1994; pp 27−112.
(22) Greenfield, M. S.; Ronemus, A. D.; Vold, R. L.; Vold, R. R.; Ellis, P. D.; Raidy, T. E. *J. Magn. Reson.* **1987**, *72*, 89–107.
(23) Hepp, M. A.; Ramamurthy, V.; Corbin, D. R.; Dybowski, C. *J. Phys. Chem.* **1992**, *96*, 2629–2632.
(24) Xiong, J.; Maciel, G. E. *J. Phys. Chem. B* **1999**, *103*, 5543–5549.
(25) Vitale, G.; Bull, L. M.; Morris, R. E.; Cheetham, A. K.; Toby, B. H.; Coe, C. G.; MacDougall, J. E. *J. Phys. Chem.* **1995**, *99*, 16087–16092.
(26) Yim, C. T.; Brown, G. R. *Langmuir* **1994**, *10*, 4195–4202.
(27) Schulz, M.; Van der Est, A.; Roessler, E.; Kossmehl, G; Vieth, H. M. *Macromolecules* **1991**, *24* (18), 5040–5045.
(28) Albunia, A. R.; Graf, R.; Guerra, G.; Spiess, H. W. *Macromol. Chem. Phys.* **2005**, *206*, 715–724.
(29) Ok, J. H.; Vold, R. R.; Vold, R. L.; Etter, M. C. *J. Phys. Chem.* **1989**, *93*, 7618–7624.
(30) Aliev, A. E.; Harris, K. D. M.; Guillaume, F. *J. Phys. Chem.* **1995**, *99*, 1156–1165.
(31) Nishikiori, S.; Kitazawa, T.; Kim, C.-H.; Iwamoto, T. *J. Phys. Chem. A* **2000**, *104*, 2591–2598.
(32) Villanueva-Garibay, J.; Muller, K. *J. Phys. Chem. B* **2004**, *108*, 15057–68.
(33) Xiong, J.; Lock, H.; Chuang, I.−S.; Keeler, C.; Maciel, G. E. *Environ. Sci. Technol.* **1999**, *33*, 2224–2233.
(34) Various experimental data for the IHSS samples is presented at www.ihss.gatech.edu.
(35) Dinar, E.; Mentel, T. F.; Rudich, Y. *Atmos. Chem. Phys.* **2006**, *6*, 5213–5224.
(36) Beshah, K.; Olejniczak, E. T.; Griffin, R. G. *J. Chem. Phys.* **1987**, *86*, 4730–4736.
(37) Eastman, M. A.; Nanny, M. A. *J. Magn. Reson.* **2007**, *184*, 302–314.
(38) Laaksonen, A.; Stilbs, P.; Wasylishen, R. E. *J. Phys. Chem.* **1998**, *108*, 455–468.
(39) Kantola, A. M.; Ahola, S.; Vaara, J.; Saunavaara, J.; Jokisaari, J. *Phys. Chem. Chem. Phys.* **2007**, *9*, 481–490.
(40) Gall, C. M.; DiVerdi, J. A.; Opella, S. J. *J. Am. Chem. Soc.* **1981**, *103*, 5039–5043.
(41) Goodwin, R. D. *J. Phys. Chem. Ref. Data* **1988**, *17*, 1541–1636.
(42) Aliev, A. E.; Harris, K. D. M. *Magn. Reson. Chem.* **1998**, *36*, 855–868.
(43) Armstrong, R. L.; Bogdan, M.; Jeffrey, K. R.; Bissonnette, C.; McCourt, F. R. W. *J. Chem. Phys.* **1993**, *99* (8), 5754–5761.
(44) Gilboa, H.; Chapman, B. E.; Kuchel, P. W. *J. Magn. Reson. A* **1996**, *119*, 1–5.
(45) Hinshaw, W. S.; Hubbard, P. S. *J. Chem. Phys.* **1971**, *54*, 428–431.
(46) Gordon, R. G. *J. Chem. Phys.* **1966**, *44*, 228–234.
(47) Chen, Y. -H.; Hwang, L. -P. *J. Phys. Chem. B* **1999**, *103*, 5070–5080.
(48) Wilson, C. L. *Nature* **1935**, *136*, 301.
(49) Chefetz, B.; Xing, B. *Environ. Sci. Technol.* **2009**, *34*, 1680–1688.
(50) Gottlieb, H. E.; Luz, Z. *Macromolecules* **1984**, *17*, 1959–1964.
(51) Mao, J.-D.; Hundal, L. S.; Thompson, M. L.; Schmidt-Rohr, K. *Environ. Sci. Technol.* **2002**, *36*, 929–936.
(52) Salloum, M. J.; Chefetz, B.; Hatcher, P. G. *Environ. Sci. Technol.* **2002**, *36*, 1953–1958.
(53) Chefetz, B.; Deshmukh, A. P.; Hatcher, P. G.; Guthrie, E. A. *Environ. Sci. Technol.* **2000**, *34*, 2925–2930.
(54) Weintraub, O.; Vega, S. *Solid State Nucl. Magn. Reson.* **1995**, *4*, 341–351.
(55) Chang, M.; Wu, S.; Chen, C. *Environ. Sci. Technol.* **1997**, *31*, 2307–2312.
(56) Sander, M.; Pignatello, J. J. *Environ. Sci. Technol.* **2005**, *39*, 7476–7484.
(57) Sander, M.; Lu, Y.; Pignatello, J. J. *Environ. Sci. Technol.* **2006**, *40*, 170–178.
(58) Lide, D. R., Ed. *CRC Handbook of Chemistry and Physics*, 88th ed.; CRC Press: Boca Raton, FL, 2007−2008.
(59) Coker, E. N.; Jia, C.; Karge, H. G. *Langmuir* **2000**, *16*, 1205–1210.
(60) Lima, C. F. R. A. C.; Sousa, C. A. D.; Rodriguez-Borges, J. E.; Melo, A.; Gomes., L. R.; Low, J. N.; Santos, L. M. N. B. F. *Phys. Chem. Chem. Phys.* **2010**, *12*, 11228–11237.
(61) Sutton, R.; Sposito, G. *Environ. Sci. Technol.* **2009**, *39* (23), 9009–9015.
(62) Gallegos, D. P.; Munn, K.; Smith, D. M.; Stermer, D. L. *J. Colloid Interface Sci.* **1987**, *119*, 127–140.